ELSEVIER

Journal of Physics and Chemistry of Solids 63 (2002) 1691–1698

JOURNAL OF PHYSICS AND CHEMISTRY OF SOLIDS

www.elsevier.com/locate/jpcs

Large supercell molecular dynamics study of defect formation in hydrogenated amorphous silicon

Charles W. Myles[a,*], Byeong C. Ha[b], Young K. Park[c]

[a]*Department of Physics, Texas Tech University, Box 41051, Lubbock, TX 79409-1051, USA*
[b]*Department of Physics, University of Texas at Arlington, Arlington, TX 76019, USA*
[c]*Semiconductor Materials Laboratory, Korea Institute of Science and Technology, Cheongryang, 130-650 Seoul, South Korea*

Received 20 June 2001; accepted 10 November 2001

Abstract

We have performed molecular dynamics simulations of the defect formation associated with the Staebler–Wronski (SW) effect in a-Si:H using 224 and 231 atom supercells and employing semiempirical Si–Si and Si–H total energy functionals. The role of hydrogen in the defect formation within the bond breaking model of the SW effect has been investigated for both large supercells. The results suggest that, within this model, H can be important in weakening the normal Si–Si bonds which break to produce defects in the SW effect.

Keywords: A. Amorphous materials; D. Defects

1. Introduction

It is well known that the electronic properties of amorphous silicon can be enhanced by adding hydrogen, which stabilizes the unsaturated dangling bonds. However, it is also believed that hydrogen might be related to the light-induced degradation of this material, which is known as the Staebler–Wronski (SW) effect [1,2].

There is some experimental evidence of a relationship between H and the SW effect in a-Si:H. For example, Bhattacharya and Mahan [3] have shown that there is a relation between the H concentration and the SW effect, Zafar and Schiff [4] have given evidence of the relation between defect density and the H concentration, and Carlson and Magee [5] have commented that the SW effect is related to the microstructure, involving the motion of H.

To our knowledge, however, there is no direct theoretical evidence that H plays a role in the defect formation associated with the SW effect. Some calculations have found, though, that H can induce defects in the material. For example, Safonov and Lightowlers [6] have suggested that defects are affected by at least three H atoms, Jones and Lister [7] have found that light induces H motion in locally strained regions and have suggested this as a cause of the SW effect, and Dersch et al. [8] have suggested that H participates in the defect formation associated with the newly created Si dangling bond in the SW effect.

There have also been experimental [9–26] and theoretical [27–36] studies of dangling bonds and H in a-Si:H which have suggested that H plays little or no role in the defect formation associated with the SW effect. One of the motivations for the present work is that, despite many years of research, the role of H in the SW effect in a-Si:H still remains controversial. In this paper, we use molecular dynamics (MD), along with the bond breaking model of the SW effect, to study this problem.

Our MD simulations were performed using 224 ($Si_{213}H_{11}$) and 231 ($Si_{211}H_{20}$) atom supercells. These were prepared (P.A. Fedders, private communication) using an ab initio pseudo-atomic orbital-based MD method [37,38]. Park and Myles (PM) [39] have performed a similar study using 60 atom supercells. The present work is an extension of this earlier study to larger supercells. In our calculations, the bond breaking model of the SW effect was simulated by applying ~2.0 eV local excitation energies to weak bonds. Both bonds which are near H's and bonds which are not near H's were studied. The simulations were performed using the PM [39–41] semiempirical total energy functional for

* Corresponding author. Tel.: +1-806-742-3767; fax: +1-806-742-1182.
E-mail address: charley.myles@ttu.edu (C.W. Myles).

0022-3697/02/$ - see front matter
PII: S0022-3697(01)00255-4

a-Si:H. In order to minimize finite size surface effects, periodic boundary conditions were employed.

There have been a number of studies of a-Si:H using MD techniques. These have considered a variety of problems and have used both tightbinding [42–44] and ab initio [33–36,45–55] methods. First principles methods have the obvious advantage of accuracy. However, they also have the disadvantage that they are usually limited to small supercells. On the other hand, tightbinding methods can more easily be applied to large supercells, but they are often less accurate than ab initio methods. The present calculations combine some of the advantages of both methods by applying a previously tested, semiempirical tightbinding total energy scheme [39–41] to large supercells, which were prepared (P.A. Fedders, private communication) using an ab initio method [37,38]. The form of the total energy used was derived from a quantum mechanical analysis and is expressed in terms of the moments of the tightbinding Hamiltonian [40,41].

Our simulation results for the investigated two large supercells suggest that H can play a crucial role in this model of the SW effect. We find that, within this supercell and bond breaking model, the SW effect can not only be caused by the mechanism of the breaking of weak Si–Si bonds, but can also be influenced by the fact that H has weakened normal Si–Si bonds. We also find that an increased H concentration can make the material more susceptible to bond breaking. These calculations thus qualitatively support both the bond breaking model of the SW effect and the idea that H plays a role in this effect.

2. Molecular dynamics and semiempirical total energy functional

In MD, the particles are given initial coordinates and momenta. Their subsequent positions are then obtained by solving the Newton's second law equations, $\vec{F}_i = m_i(\mathrm{d}^2\vec{r}_i/\mathrm{d}t^2)$ for each particle. In semiempirical methods, the forces acting on an atom at position $\vec{r}_i$ are obtained from interatomic potentials or from the derivative $\vec{F}_i = -\vec{\nabla}_i E_{\mathrm{tot}}$, where E_{tot} is the total energy of the system.

In this paper, the forces are obtained from a semiempirical total energy functional E_{tot} which is derived from the quantum mechanical electronic structure. This functional is based on the moment method discussed by Carlsson [56] and was developed for Si systems by Carlsson, Fedders and Myles (CFM) [57] and for Si–H systems by PM [40,41]. This formalism begins with a one-electron, tightbinding Hamiltonian of the form

$$H = \sum_i \sum_\alpha E^\alpha(i) + \sum_{i,j} \sum_{\alpha,\beta} h_{ij}^{\alpha,\beta} |i,\alpha><j,\beta|, \tag{1}$$

where i,j represent atomic positions, α,β are localized s, p_x, p_y, and p_z orbitals, and $E^\alpha(i)$ is the αth orbital energy at site i. The couplings $h_{ij}^{\alpha,\beta}$ are assumed to have two center forms with angular dependences given by the Slater–Koster relations [58,59]. The Si–Si couplings in the Hamiltonian are determined by the functions $h_{ij}^{ss\sigma}$(Si), $h_{ij}^{sp\sigma}$(Si), $h_{ij}^{pp\sigma}$(Si), and $h_{ij}^{pp\pi}$(Si). For Si–H interactions, the couplings are $h_{ij}^{\alpha,\beta}$(H), and $h_{ij}^{sp\sigma}$(H). For $E^\alpha(i)$, the s and p atomic energies of Si and the s atomic energy of H are used. The semiempirical parameters which enter the $h_{ij}^{\alpha,\beta}$, as well as the functional forms of these quantities may be found in Refs. [40,41,57].

The total energy functional contains terms which come from two, three, and four-body interactions [40,41,56,57].

It has the schematic form

$$E_{\mathrm{tot}} = \frac{1}{2}\sum_{i,j} V^{\mathrm{rep}}(i,j) + E_{\mathrm{el}}^{(2)} + E_{\mathrm{dip}} + E_{\mathrm{el}}^{(4)}. \tag{2}$$

Here, $E_{\mathrm{el}}^{(2)}$ is a geometrical, two-body path term obtained from the second moment matrix $\mu_2(i)$ of the Hamiltonian, Eq. (1). This matrix contains information about the radial and angular distribution of the neighbors of atom i. The $E_{\mathrm{el}}^{(4)}$ term is obtained from the fourth moment $\mu_4(i)$ of the Hamiltonian. This term is a geometrical four-body path term multiplied by an environmental factor. The E_{dip} term is the self-energy of the electrostatic dipole created when an atom is placed in an environment lacking inversion symmetry. The term V^{rep} represents repulsive two-body potentials between the nuclei and simulates the repulsion resulting from the overlap between the occupied electron states on neighboring sites. There are two types of repulsive potentials. These are $V_{\mathrm{Si}}^{\mathrm{rep}}(i,j)$ and $V_{\mathrm{H}}^{\mathrm{rep}}(i,j)$, for Si–Si and Si–H interactions, respectively. The explicit representations of each of the energy terms in Eq. (2) as functions of the moments of the Hamiltonian are given in Refs. [40,41,57].

We note that, while this total energy formulation begins with a tightbinding Hamiltonian which contains only two-body terms, the resulting total energy functional is more general than this. In particular, it does *not* have the form found in most tightbinding MD schemes [42–44,60–63]. Further, due to the representation of each term of Eq. (2) as a functional of the moments of the Hamiltonian, it includes environmental effects in up to four atom paths beginning and ending on a given atomic site [40,41,56,57].

The Hellmann–Feynman theorem [64–68] is used to evaluate the forces we use in our MD simulations. According to this theorem, if the total energy E_{tot} is known, forces can be evaluated by taking the derivative as $\vec{F}_i = -\vec{\nabla}_i E_{\mathrm{tot}}$. The forces depend on the derivatives of $h_{ij}^{\alpha\beta}$ and $V^{rep}(i,j)$. For the derivatives of the radial parts, $h(r)$, of these functions, we assume that $(\partial h(r)/\partial r) = 0$ for $r > r_{\max}$, where $r_{\max}$ is a cutoff radius. Following previous work [40,41,57], in our simulations, a value of $r_{\max} = 4.4$ Å has been chosen. At equilibrium, the total force $\vec{F}_i$ equals zero for each atom.

After a local disturbance, the system will relax to an equilibrium state, which can be found by quenching. The system is quenched by setting all velocities to zero. In our

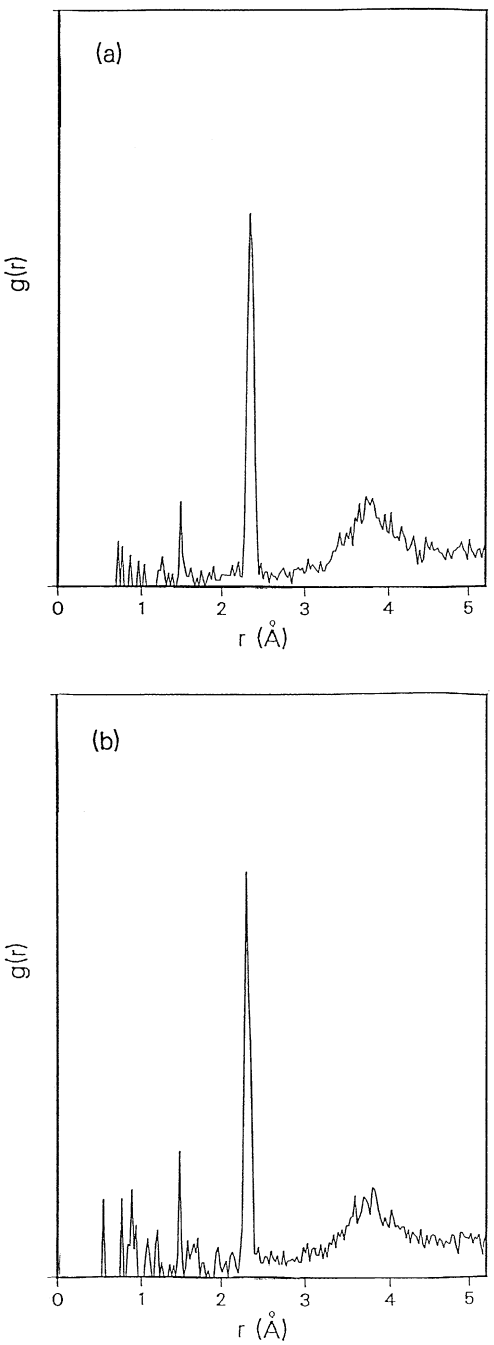

Fig. 1. The radial distribution functions $g(r)$ for the supercells used as the initial configurations for the MD simulations. (a) 224 atom supercell (Model 1: $Si_{213}H_{11}$), and (b) 231 atom supercell (Model 2: $Si_{211}H_{20}$).

calculations, we use the very efficient power quenching scheme. In this method, individual velocity components are quenched if the directions of the forces are opposite to the directions of the velocities.

3. MD simulations

3.1. Supercell models

Both 224 ($Si_{213}H_{11}$) and 231 ($Si_{211}H_{20}$) atom supercell models were employed as the initial configurations in our simulations. These were prepared (P.A. Fedders, private communication) using an ab initio pseudo-atomic orbital MD technique [37,38].

In the initial state, the 224 atom supercell (Model 1) has one dihydride and nine monohydride Si's, 4.9 at.% H, one dangling bond, and no floating bonds. Its density is 2.30 g/cm^3 and its average Si–Si and Si–H bond lengths are 2.359 and 1.502 Å, respectively. Fig. 1(a) shows the radial distribution function $g(r)$ for this supercell. The peak at 1.502 Å indicates the average distance between Si atoms and their nearest H neighbors. The peak at 2.359 Å indicates the average Si–Si nearest-neighbor bond length. This compares favorably with the 2.35 Å bond length in crystalline Si. The broad peak centered around 3.8 Å represents the distribution of second-nearest-neighbor Si–Si distances.

The initial state for the 231 atom supercell (Model 2) has two dihydride and 16 monohydride Si's, 8.7 at.% H, two dangling bonds, and two floating bonds. Its density is 2.27 g/cm^3 and its average Si–Si and Si–H bond lengths are 2.358 and 1.504 Å. Fig. 1(b) shows the radial distribution function $g(r)$ for this supercell. The peaks centered at 1.504, 2.358 and 3.8 Å represent the distribution of Si–H bond lengths, Si–Si nearest-neighbor bond lengths, and Si–Si second-neighbor distances, respectively.

3.2. Simulation details

A simple, computationally feasible way to simulate the recombination energy transfer of an excited electron–hole pair in the SW effect is to create a local excitation energy ('hot spot') at a bond. This is the method we use to simulate the bond breaking model of the SW effect. In our simulations, a local excitation energy of ~2.0 eV is applied to the bond between two atoms. In the cases considered, we have found that an excitation of this size is often near the critical energy for bond breaking. A pseudo-random number generator is used to assign the initial velocities of the two atoms. For models 1 and 2, we have performed simulations for (i) normal Si–Si bonds with no neighboring H, (ii) weak Si–Si bonds with no neighboring H, (iii) normal Si–Si bonds with neighboring H, and (iv) weak Si–H bonds.

In our simulations, before a local excitation energy was applied, the samples were first relaxed for 150 fs using forces obtained from the CFM [57] and PM [40,41] semi-empirical total energy functionals. After relaxation, they were quenched.

3.3. Model 1: 224 atom supercell ($Si_{213}H_{11}$)

For this supercell, simulations were carried out for normal Si–Si bonds with no neighboring H, for weak Si–Si bonds

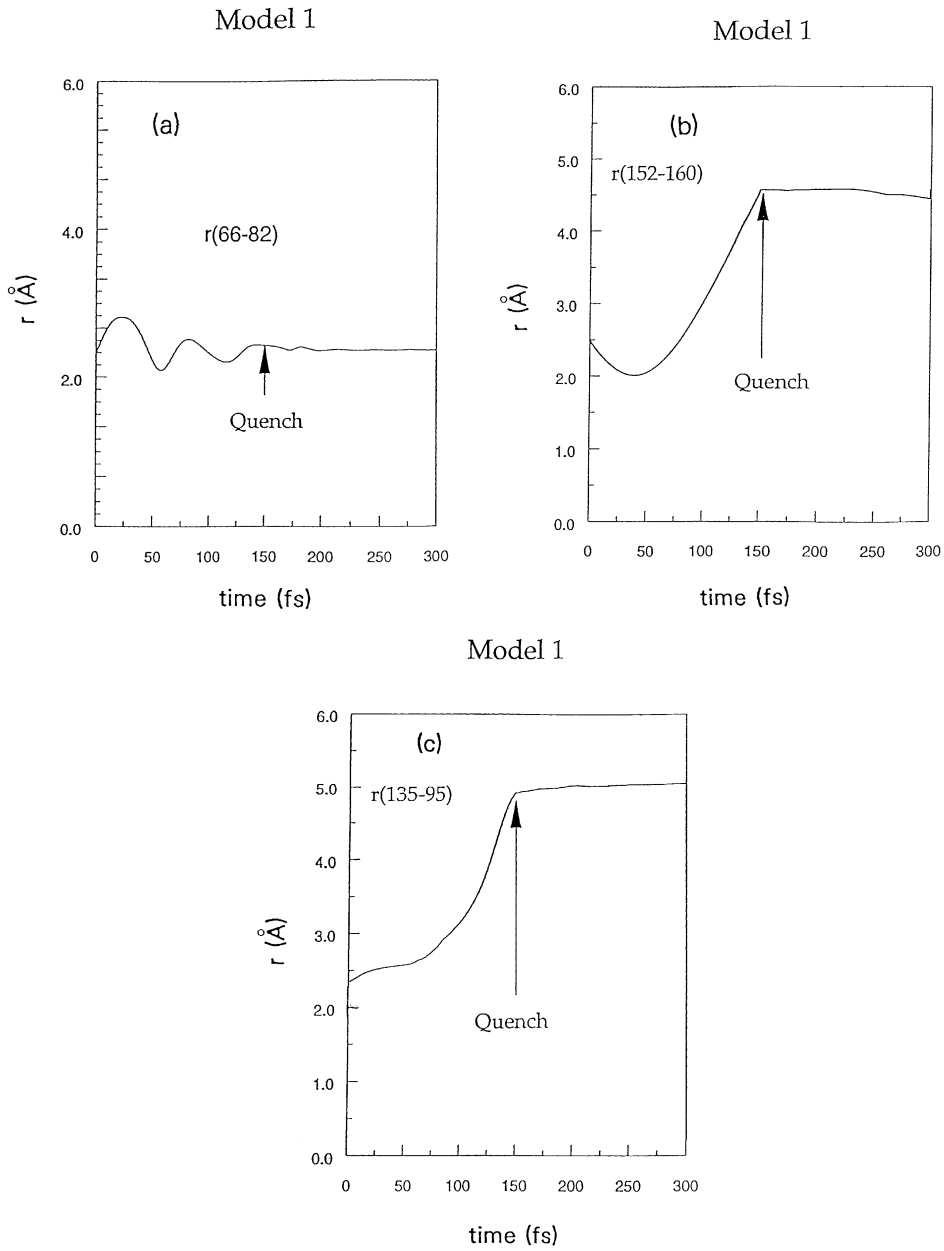

Fig. 2. The post-excitation time dependences of various bond lengths for Model 1 ($Si_{213}H_{11}$). (a) Normal Si–Si bond (66–82) with no neighboring H after the application of a 2.0 eV excitation. Clearly, the bond is not broken. (b) Weak Si–Si bond (152–160) with no neighboring H after a 2.0 eV excitation. The bond is clearly broken after about 100 fs. (c) Normal Si–Si bond (135–95) near a monohydride Si after a 2.0 eV excitation. Clearly, the bond is broken after about 100 fs.

with no neighboring H, and for normal Si–Si bonds near monohydride Si's. Typical, representative results for the post-excitation time dependence of a bond length are shown in Fig. 2(a) for a normal Si–Si bond, in Fig. 2(b) for a weak Si–Si bond with no neighboring H, and in Fig. 2(c) for a normal Si–Si bond near a monohydride Si. In each of the three cases, an excitation of 2.0 eV has been applied.

In Fig. 2(a), we show the time dependence after excitation of the bond length for a normal Si–Si bond (bond 66–82). This bond has no neighboring H. The initial bond length is 2.316 Å. It can be seen that this bond length oscillates with

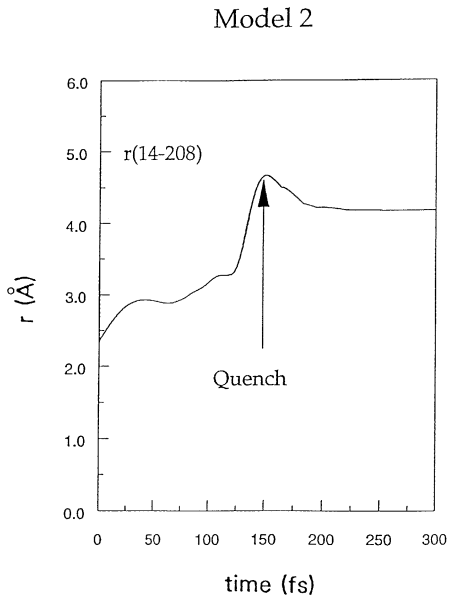

Fig. 3. The post-excitation time dependence of a normal Si–Si bond (14–208) for Model 2 ($Si_{211}H_{20}$) after application of a 2.0 eV excitation. This bond is near a dihydride Si (atom 14). Clearly, the bond is broken after about 50 fs.

decreasing amplitude for 150 fs, after which quenching took place. Clearly, no bond breaking is observed.

In Fig. 2(b), we show the post-excitation time dependence of the bond length of a weak Si–Si bond (bond 152–160) with no neighboring H. The initial bond length is 2.49 Å. In our calculations, if the bond length is greater than 2.8 Å, it is considered broken. This figure thus shows that the bond is broken after about 100 fs, as is indicated by the abrupt increase in bond length after that time.

In Fig. 2(c), we show the time dependence of the bond length after excitation of a normal Si–Si bond (bond 135–95) near a monohydride Si. The initial bond length is 2.366 Å. Clearly, the bond is again broken after about 100 fs. The bond breaking in this case is thus very similar to that for a weak Si–Si bond (Fig. 2(b)). These and similar results thus suggest that the presence of H can weaken a normal Si–Si bond.

3.4. Model 2: 231 atom supercell ($Si_{211}H_{20}$)

In our simulations for this supercell, the same procedures as for Model 1 were used. In this case, we particularly focused on normal Si–Si bonds near hydrogens. Typical, representative results for the post-excitation time dependence of a bond length are shown in Fig. 3. This figure shows that a normal Si–Si bond (14–208) near a dihydride Si (atom 14) is broken by a 2.0 eV local excitation. We note that, in this case, the bond is broken rather rapidly, in ~50 fs, in contrast to the ~100 fs bond breaking times we found for the cases shown in Fig. 2. These and similar

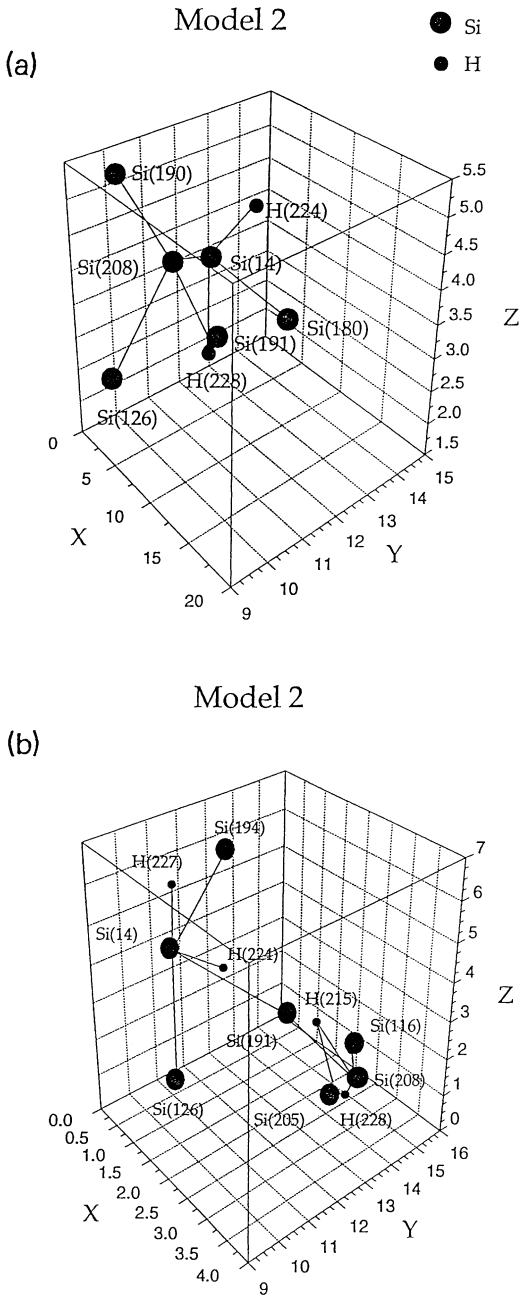

Fig. 4. A schematic illustration of bond breaking caused by the application of a 2.0 eV excitation to the normal bond between two Si atoms (atoms 14 and 208) in Model 2 ($Si_{211}H_{20}$). Atom 14 is a dihydride Si. (The post-excitation time dependence of the bond length is shown in Fig. 3.) Note that this is a two-dimensional illustration of a three-dimensional process. The coordinates *X*, *Y*, and *Z* are all in Å. (a) Initial configuration. (b) Final configuration. After bond 14–208 is broken, two H-centered Si bonds and a Si-centered bond are formed.

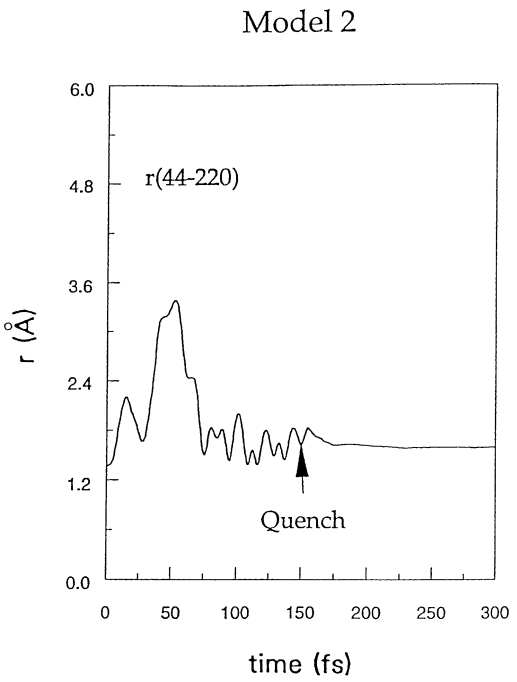

Fig. 5. The post-excitation time dependence of a Si–H bond (44–220) for Model 2 ($Si_{211}H_{20}$) after application of a 2.0 eV excitation. For about ~50 fs, the bond appears to 'break'. It then appears to 're-heal' as it begins to oscillate about a constant value. Thus, this bond is not (permanently) broken by this excitation energy.

results indicate again that H's near a normal Si–Si bond can weaken it. Furthermore, when such a bond is broken by the excitation, the structure near it is changed, creating dangling bonds as well as floating bonds. For bond 14–208, the initial and final local atomic configurations are shown schematically in Fig. 4(a) and (b).

From Fig. 4(a), it can be seen that, in the initial configuration, atom 14 is a dihydride Si. The initial bond length between atoms 14 and 208 was 2.282 Å. As may be seen from Fig. 4(b), after the local excitation between Si atoms 14 and 208, the bond is broken and these two atoms are separated by a long distance. In the final configuration, Si atom 191 is centered between Si atoms 14 and 208, thus forming a floating bond, and H atoms 215 and 228 are centered between Si atoms 205 and 208, forming bond-centered H configurations. Hydrogen atom 228, which was bonded to Si atom 14, has moved and has bonded to Si atom 208 after the excitation. Also, a new H (atom 227) is now bonded to Si atom 14. Two H atoms, which were not found in the initial configuration, are bonded to Si atom 208. These results thus clearly show that, in this case, the excitation energy has caused a H rearrangement.

Typical, representative results for the application of a local excitation to a Si–H bond are shown in Fig. 5. There, we show the time dependence of the bond length after a 2.0 eV excitation is applied to the bond between Si atom 44 and H atom 220. The initial bond length was 1.52 Å. From the figure, for about ~50 fs, the bond appears to 'break'. It then appears to 're-heal' again as it begins to oscillate about a constant value of about 1.55 Å. This figure thus shows that this bond is not (permanently) broken by a 2.0 eV local excitation energy. We have found in other simulations that, for this excitation energy, such bond breaking happens on Si–Si bonds, but not on Si–H bonds.

4. Discussion

In carrying out our simulations, we have found that, in the 231 atom supercell (Model 2), which has the higher H concentration of the two supercells used, Si–Si bonds are more easily broken than in the lower H concentration, 224 atom supercell (Model 1). This implies that the supercell with the higher H concentration is less stable against local excitations than that with the smaller concentration. The increasing ease of bond breaking thus correlates with an increase in H content in the supercell.

Bhattacharya and Mahan [3] have found in infrared absorption experiments that samples with more bonded H show an increase in the SW effect. In addition, constant photocurrent measurements by Johnson et al. [69] have demonstrated that the stability of the electronic properties of a-Si:H can be affected by H migration and bonding. These results are qualitatively consistent with our simulation results. We also find that the SW effect is probably not due to the breaking of Si–H bonds.

Our results are also consistent with those of other experiments. For example, Hirabayashi et al. [70] have suggested that a possible site for a dangling bond created by illumination may be a Si–Si bond next to a Si–H bond. They argue that as the Si–H bond strain is stronger than the Si–Si bond strain, and H is more electronegative than Si, the electrons at a central Si atom are more localized towards the Si–H bond. Thus, they conclude, in qualitative agreement with our results, that a normal Si–Si bond near a H is more easily broken than a normal Si–Si bond with no H nearby.

Stutzmann et al. [71] have suggested that the defect state associated with the SW effect is linked to stress. They found that the number of metastable defects increases with the average stress and that there is thus a recombination-induced breaking of weak bonds. We suggest that this stress has a close relation with the Si–H bond strain. Dangling bonds are associated with microstructural defects as a result of weaker Si–Si bonds, where monohydride and dihydride bonding dominates. Local rearrangements of H atoms, such as those found in our simulations, can help to explain the observed defect metastability. In our simulations of the bond breaking model, we find that the magnitude and kinetic behavior of the SW effect can be different in the cases of small and large H concentrations, as is consistent with the experimental evidence.

We have also shown that, within the bond breaking model

of the SW effect, the broken bonds can rebond with H or Si. In their calculations, Dersch et al. [8] have suggested that the dangling bond pairs created by Si–Si bond breaking can become spatially separated due to structural relaxation. A question was whether local rearrangements of H atoms are necessary to explain the observed metastability of the light-induced defects, or whether structural relaxation of Si atoms alone is sufficient. Our calculations suggest that the SW effect is associated not only with structural relaxation of the Si atoms, but also with local rearrangements of H atoms.

It is well known that there is a complex relationship between H and the Si bonding structure. The passivation of dangling bonds is the primary beneficial effect of H in a-Si:H. However, our calculations suggest that H also can cause reconstruction of the network, breaking and removing weak Si–Si bonds, as has also been suggested by others [72,73].

The release of H into the Si network also promotes the reconstruction of the Si bonds. As the H concentration increases, the defect density increases, showing the connection between the H bonding and the defect states. In our calculations, more dangling bonds are created after a local excitation, there are extensive reconstructions of the network, and a normal Si–Si bond is more easily broken when H is nearby. We thus suggest that Si–Si bonds near H are thus weakened by the Si–H forces, resulting in easier bond breaking by illumination.

5. Conclusions

We have used MD simulations to study defect formation within the bond breaking model of the SW effect and have studied the role H plays in this model. Both 214 and 231 atom supercells, prepared (P.A. Fedders, private communication) using an ab initio method [37,38], have been used in this study. The semiempirical total energy functionals of CFM [57] and of PM [40,41] have been used to model the Si–Si and Si–H interatomic forces. Representative simulation results have been presented in Figs. 2–5.

Important and interesting phenomena were found in both supercells. We have found that normal Si–Si bonds near monohydride and dihydride Si's are more easily broken by a $\sim$2.0 eV local excitation energy than normal bonds with no H nearby. We find, however, that initially weak Si–Si bonds with no H nearby are as easily broken as the normal bonds which are near H. We thus suggest that the presence of H weakens a normal bond, making it more susceptible to bond breaking by a local excitation. We also have found that such bond breaking results in dangling bonds and rearrangement of the nearby Si and H atoms. This suggests that H may play a role in defect formation in the SW effect.

Earlier, PM [39] performed 60 atom supercell MD simulations, using the same total energy functional as was employed here, to study the role of H in the defect formation associated with the SW effect (within the bond breaking model). We note that, in contrast to our results, their results suggest that H probably is not involved in the SW effect. Other than the supercell size, the only difference between the PM study and the present study is in how the supercells used for the initial conditions were prepared. In the PM study [39], supercells prepared by Guttman and Fong [74] were used for the initial conditions. We thus suggest that, in MD simulations, the role H plays in the bond breaking model of the SW effect in a-Si:H may depend crucially on the initial conditions in the supercell sample used.

A weakness both of the present study and of the earlier study by PM [39] is that only *local* bond breaking has been considered in both cases. In actual SW effect experiments, the electrons which are liberated by bond breaking are excited to low-lying conduction band states and these are likely not localized on a single bond. The inclusion of such *non-local* effects would require a fully quantum mechanical study and is thus beyond the capability of the present model.

Another weakness of the present study is that we have performed our calculations on only a few supercell samples and have presented only representative results here. Thus, our conclusions, while plausible based on the results shown, are not backed up by strong statistics. Many more supercell samples would need to be studied in order for our conclusions to be placed on a firmer foundation.

Acknowledgements

We thank the BMDO for a grant (No. N00014-93-1-0518) through ONR and the Texas Advanced Research Program for a grant (No. 003644-047), both of which supported this work. We thank P.A. Fedders for preparing the large supercells used in this study, for helpful comments, and for a critical reading of the manuscript.

References

[1] D.L. Staebler, C.R. Wronski, Appl. Phys. Lett. 31 (1977) 292.
[2] D.L. Staebler, C.R. Wronski, J. Appl. Phys. 51 (1980) 3262.
[3] E. Bhattacharya, A.H. Mahan, Appl. Phys. Lett. 52 (19) (1988) 1587.
[4] S. Zafar, E.A. Schiff, Phys. Rev. Lett. 66 (1991) 1493.
[5] D.E. Carlson, C.W. Magee, Appl. Phys. Lett. 33 (1978) 1581.
[6] A.N. Safonov, E.C. Lightowlers, Mat. Sci. Forum 143–147 (1994) 903.
[7] R. Jones, G.M.S. Lister, Phil. Mag. 61 (1990) 881.
[8] H. Dersch, J. Stuke, J. Beichler, Appl. Phys. Lett. 38 (6) (1981) 456.
[9] P. Agarwal, S.C. Agarwal, Phil. Mag. B 80 (2000) 1327.
[10] K. Luterova, I. Pelant, P. Horath, Phil. Mag. B 80 (2000) 1811.
[11] M.H. Chu, C.H. Wu, J. Phys. Chem. B 104 (2000) 3924.
[12] J. Cui, S.F. Yoon, J. Appl. Phys. 89 (2001) 6153.
[13] U.K. Das, T. Yasuda, S. Yamasaki, Phys. Rev. B 63 (2001) 245204.

[14] K.C. Palinginis, J.D. Cohen, S. Guha, J.C. Yang, Phys. Rev. B 63 (2001) 201203.
[15] T. Umeda, S. Yamasaki, J. Isoya, K. Tanaka, Phys. Rev. B 62 (2000) 15702.
[16] D. Han, J. Baugh, G. Yue, Q. Wang, Phys. Rev. B 62 (2000) 7169.
[17] R.E. Norberg, D.J. Leopold, P.A. Fedders, J. Non-Cryst. Solids 230 (1998) 124.
[18] L.S. Sidhus, T. Kosteski, S. Zukotynski, N.P. Kherani, W.T. Shmayda, Appl. Phys. Lett. 74 (1999) 3975.
[19] H. Touir, K. Zellama, J.F. Morhange, Phys. Rev. B 59 (1999) 10076.
[20] M.S. Brandt, M.W. Bayerel, M. Stutzmann, J. Non-Cryst. Solids 230 (1998) 343.
[21] D. Kwon, C.C. Chen, J.D. Cohen, H.C. Jin, E. Holler, I. Robertson, J. Abelson, Phys. Rev. 60 (1999) 4442.
[22] T. Umeda, S. Yamasaki, J. Isoya, K. Tanaka, Phys. Rev. B 59 (1999) 4849.
[23] S. Yamasaki, T. Umeda, J. Isoya, J. Zhou, K. Tanaka, J. Non-Cryst. Solids 230 (1998) 332.
[24] T. Umeda, S. Yamasaki, J. Isoya, A. Matsuda, K. Tanaka, J. Non-Cryst. Solids 230 (1998) 353.
[25] J. Isoya, S. Yamasaki, A. Matsuda, K. Tanaka, Phil. Mag. B 69 (1994) 263.
[26] Q. Zhang, N. Nishino, H. Takashima, M. Kumeda, T. Shimizu, Jpn. J. Appl. Phys. 35 (1996) 4409.
[27] M. Peressi, M. Forniari, A. Baldereschi, Phil. Mag. 80 (2000) 515.
[28] A.M. Ferreira, H.A. Kurtz, S.P. Karna, J. Phys. Chem. A 104 (2000) 3924.
[29] E. Kim, Y.H. Lee, C. Chen, T. Pang, Phys. Rev. B 59 (1999) 2713.
[30] J.L. Feldman, P.B. Allen, S.R. Bickman, Phys. Rev. B 59 (1999) 3551.
[31] K. Nakajima, K. Miyazaki, H. Koinuma, K. Sato, J. Appl. Phys. 84 (1998) 607.
[32] K. Takeda, H. Hikita, Y. Kimura, M. Yamaguchi, K. Morigaka, Jpn. J. Appl. Phys. 36 (1997) 991.
[33] P.A. Fedders, D.A. Drabold, Phys. Rev. B 53 (1996) 3841.
[34] P.A. Fedders, D.A. Drabold, Phys. Rev. B 47 (1993) 13277.
[35] H.M. Banz, T. Unold, P.A. Fedders, J. Non-Cryst. Solids 200 (1996) 535.
[36] H.M. Branz, Phys. Rev. B 59 (1999) 5498.
[37] O.F. Sankey, D.J. Niklewski, Phys. Rev. B 40 (1989) 3979.
[38] O.F. Sankey, D.J. Niklewski, D.A. Drabold, J.D. Dow, Phys. Rev. B 41 (1990) 12750.
[39] Y.K. Park, C.W. Myles, Phys. Rev. B 51 (1995) 1671.
[40] Y.K. Park, PhD Dissertation, Texas Tech University, 1994.
[41] Y.K. Park, C.W. Myles, Phys. Rev. B 48 (1993) 17086.
[42] P. Klein, H.M. Urbassek, T. Frauenheim, Phys. Rev. B 60 (1999) 5478.
[43] D.E. Boucher, G.G. DeLeo, Phys. Rev. B 50 (1994) 5247.
[44] G. Panzarini, L. Colombo, Phys. Rev. Lett. 73 (1994) 1636.
[45] M. Ishmaru, J. Phys. Condensed Matter 13 (2001) 4181.
[46] B. Tuttle, J.B. Adams, Phys. Rev. B 53 (1996) 16256.
[47] B. Tuttle, J.B. Adams, Phys. Rev. B 57 (1998) 12859.
[48] S.M. Nakhmanson, D.A. Drabold, Phys. Rev. B 58 (1998) 15325.
[49] P.A. Fedders, D.A. Drabold, S.M. Nakhmanson, Phys. Rev. B 58 (1998) 15624.
[50] C.G. Van de Valle, Phys. Rev. B 49 (1994) 4579.
[51] N. Mousseau, L.J. Lewis, Phys. Rev. B 43 (1991) 9810.
[52] F. Buda, G.L. Chiarotti, R. Car, M. Parrinello, Phys. Rev. B 44 (1991) 5908.
[53] J.M. Holender, G.J. Morgan, R. Jones, Phys. Rev. B 47 (1993) 3391.
[54] L.J. Lewis, N. Mousseau, Computat. Mater. Sci. 12 (1998) 210.
[55] M. Durandurdu, D.A. Drabold, N. Mousseau, Phys. Rev. B 62 (2000) 15307.
[56] A.E. Carlsson, in: D. Turnbull, H. Ehrenreich (Eds.), Solid State Physics: Advances in Research and Applications, 43, Academic Press, New York, 1990.
[57] A.E. Carlsson, P.A. Fedders, C.W. Myles, Phys. Rev. B 41 (1990) 1247.
[58] J.C. Slater, G.F. Koster, Phys. Rev. 94 (1954) 1498.
[59] W.A. Harrison, Electronic Structure and the Properties of Solids, Freeman, New York, 1980.
[60] I. Kwon, R. Biswas, C.M. Soukoulis, Phys. Rev. B 45 (1992) 3332.
[61] B.J. Min, Y.H. Lee, C.Z. Wang, C.T. Chan, K.M. Ho, Phys. Rev. B 45 (1992) 6839.
[62] E. Kim, Y.H. Lee, Phys. Rev. B 49 (1994) 1743.
[63] J.M. Holender, G.J. Morgan, J. Phys. Condens. Matter 4 (1992) 4473.
[64] H. Hellmann, Einfuhrung in die Quantumchemie, Franz Deutsche, Leipzig, 1937.
[65] R.P. Feynman, Phys. Rev. 56 (1939) 340.
[66] J.I. Musher, J. Chem. Phys. 43 (1965) 2145.
[67] B.M. Deb, Rev. Mod. Phys. 45 (1973) 22.
[68] W. Pauli, Handbuch der Physik, Springer, Berlin, 1933.
[69] N.M. Johnson, C.E. Nebel, P.V. Santos, W.B. Jackson, R.A. Street, K.S. Stevens, J. Walker, Appl. Phys. Lett. 59 (12) (1991) 1443.
[70] I. Hirabayashi, K. Morigaki, S. Nitta, Jpn. J. Appl. Phys. 19 (1980) L357.
[71] M. Stutzmann, W.B. Jackson, C.C. Tsai, Phys. Rev. B 32 (1985) 23.
[72] R.A. Street, Hydrogenated Amorphous Silicon, Cambridge University Press, New York, 1991.
[73] J. Kakalios, in: J.I. Pankove, N.M. Johnson (Eds.), Hydrogen in Semiconductors, Semiconductors and Semimetals, vol. 34, Academic Press, New York, 1991 Chapter 12.
[74] L. Guttman, C.Y. Fong, Phys. Rev. B 26 (1982) 6756.